© 2016. Published by The Company of Biologists Ltd | Development (2016) 143, 2325-2333 doi:10.1242/dev.136499

RESEARCH ARTICLE

The tyrosine kinase FER is responsible for the capacitation-associated increase in tyrosine phosphorylation in murine sperm

Antonio Alvau[1,*], Maria Agustina Battistone[2,*], Maria Gracia Gervasi[1], Felipe A. Navarrete[1], Xinran Xu[3], Claudia Sánchez-Cárdenas[4], Jose Luis De la Vega-Beltran[4], Vanina G. Da Ros[2], Peter A. Greer[5], Alberto Darszon[4], Diego Krapf[3], Ana Maria Salicioni[1], Patricia S. Cuasnicu[2] and Pablo E. Visconti[1,‡]

ABSTRACT

Sperm capacitation is required for fertilization. At the molecular level, this process is associated with fast activation of protein kinase A. Downstream of this event, capacitating conditions lead to an increase in tyrosine phosphorylation. The identity of the tyrosine kinase(s) mediating this process has not been conclusively demonstrated. Recent experiments using stallion and human sperm have suggested a role for PYK2 based on the use of small molecule inhibitors directed against this kinase. However, crucially, loss-of-function experiments have not been reported. Here, we used both pharmacological inhibitors and genetically modified mice models to investigate the identity of the tyrosine kinase(s) mediating the increase in tyrosine phosphorylation in mouse sperm. Similar to stallion and human, PF431396 blocks the capacitation-associated increase in tyrosine phosphorylation. Yet, sperm from *Pyk2*$^{-/-}$ mice displayed a normal increase in tyrosine phosphorylation, implying that PYK2 is not responsible for this phosphorylation process. Here, we show that PF431396 can also inhibit FER, a tyrosine kinase known to be present in sperm. Sperm from mice targeted with a kinase-inactivating mutation in *Fer* failed to undergo capacitation-associated increases in tyrosine phosphorylation. Although these mice are fertile, their sperm displayed a reduced ability to fertilize metaphase II-arrested eggs *in vitro*.

KEY WORDS: FER, Capacitation, Tyrosine phosphorylation

INTRODUCTION

Mammalian sperm acquire fertilization competence in the female tract in a process known as capacitation. Capacitation is associated with changes in motility pattern (e.g. hyperactivation) and prepares sperm to undergo acrosomal exocytosis. At the molecular level, one of the first events is a fast HCO_3^--dependent stimulation of cAMP synthesis by the atypical soluble adenylyl cyclase ADCY10 (sAC) (Buck et al., 1999). The increase in cAMP stimulates protein kinase A (PKA), which activates a series of pathways and coincides with increased protein tyrosine phosphorylation (Harrison, 2004). Since our first reports in 1995 (Visconti et al., 1995a,b), the increase in tyrosine phosphorylation has been used as an endpoint of capacitation in sperm from many species (Baldi et al., 2002; Ficarro et al., 2003; Ijiri et al., 2012; Jagan Mohanarao and Atreja, 2011; Roy and Atreja, 2008; Signorelli et al., 2012). However, the identity of the protein tyrosine kinase(s) responsible for this signaling event has remained elusive. A list of potential candidate kinases has emerged based on pharmacological and immunological evidence. Among these candidates, the most relevant were SRC (Baker et al., 2006; Krapf et al., 2010; Varano et al., 2008), FYN (Luo et al., 2012), ABL (Baker et al., 2009), and both members of the focal adhesion kinase (FAK) family, FAK and proline-rich tyrosine kinase 2 (PYK2; also known as PTK2B) (Battistone et al., 2014; Gonzalez-Fernandez et al., 2013). All these enzymes were shown to be present in sperm and, furthermore, the increase in tyrosine phosphorylation was reduced or completely obliterated when treated with inhibitors against their respective activities. Pharmacological inhibitors can be excellent tools to intervene in particular cellular processes with accurate temporal precision. However, small molecule inhibitors often have off-target effects that confound identification of candidate enzymes involved in specific processes. Therefore, to identify conclusively the tyrosine kinase(s) responsible for capacitation, genetic approaches are preferred.

In the present work, we show that PF431396, a commercially available inhibitor of FAK and PYK2 tyrosine kinases, but not PF573228, which has higher specificity for FAK than for PYK2, blocks the capacitation-associated increase in tyrosine phosphorylation without affecting the upstream phosphorylation of PKA substrates. Yet, sperm from *Pyk2*$^{-/-}$ mice display normal capacitation-associated increases in tyrosine phosphorylation. These observations argue against a role for either PYK2 or FAK in this process, and suggest that PYK2 inhibitors are acting on a different tyrosine kinase(s) during sperm capacitation. Among the candidates, FER has been recently shown to be phosphorylated on tyrosine residues during capacitation (Chung et al., 2014). Here, we show that: (1) FER and its testis-specific splicing variant FERT are present in mature murine sperm; (2) FER enzymatic activity can be inhibited by PF431396 with an IC_{50} comparable to that for PYK2; and (3) sperm from mice targeted with a kinase-inactivating mutation in *Fer* (*Fer*$^{DR/DR}$) do not display capacitation-associated increases in tyrosine phosphorylation. Interestingly, *Fer*$^{DR/DR}$ mice are fertile, but their sperm are deficient in their ability to fertilize metaphase II-arrested eggs *in vitro*. Altogether, these experiments conclusively demonstrate FER involvement in the regulation of tyrosine phosphorylation during capacitation. In addition, they strongly suggest that the increase in tyrosine phosphorylation accompanying capacitation is not essential for animal fertility and challenge the current paradigm of sperm capacitation.

[1]Department of Veterinary and Animal Science, Integrated Sciences Building, University of Massachusetts, Amherst, MA 01003, USA. [2]Instituto de Biología y Medicina Experimental (IBYME-CONICET), Buenos Aires C1428ADN, Argentina. [3]Department of Electrical and Computer Engineering and School of Biomedical Engineering, Colorado State University, Fort Collins, CO 80521, USA. [4]Departamento de Genética del Desarrollo y Fisiología Molecular, IBT-UNAM, Cuernavaca 62210, México. [5]Department of Pathology and Molecular Medicine, Queen's University, Kingston, Ontario, Canada, K7L 3N6.
*These authors contributed equally to this work

[‡]Author for correspondence (pvisconti@vasci.umass.edu)

P.E.V., 0000-0001-9320-7518

Received 17 February 2016; Accepted 12 May 2016

Development (2016) 143, 2325-2333 doi:10.1242/dev.136499

RESULTS

Members of the FAK tyrosine kinase family are present in murine sperm but do not participate in the capacitation-associated increase in tyrosine phosphorylation

Our recent work using human sperm (Battistone et al., 2014) as well as previous work from Hinrichs' group in stallion sperm (Gonzalez-Fernandez et al., 2013) suggested a role for FAK tyrosine kinase family members in the increase of protein tyrosine phosphorylation that accompanies sperm capacitation. These conclusions were based on the use of anti-phosphopeptide antibodies that recognize active forms of these enzymes and on the use of PF431396, a tyrosine kinase inhibitor considered to be most active against members of the FAK kinase subfamily. Similar to observations in horse (Gonzalez-Fernandez et al., 2013) and human (Battistone et al., 2014) sperm, the increase of tyrosine phosphorylation in murine sperm was inhibited in a dose-dependent fashion by PF431396, with an EC_{50} of ~1 µM (Fig. 1A, upper panel). However, unlike the SRC inhibitors SU6656 and SKI606 (Baker et al., 2006), PF431396 did not block phosphorylation of PKA substrates, suggesting that its inhibitory effect is downstream of PKA activation (Fig. 1A, lower panel). This hypothesis is consistent with results indicating that PF431396 blocks tyrosine phosphorylation (Fig. 1B, upper panel) without inhibiting phosphorylation of PKA substrates, even when sperm are incubated in the presence of cAMP agonists (e.g. dbcAMP and IBMX) (Fig. 1B, lower panel).

We have previously shown that members of the SRC kinase family affect the increase in tyrosine phosphorylation indirectly by downregulation of Ser/Thr phosphatases (Krapf et al., 2010). Therefore, the effect of SRC family kinase inhibitors such as SU6656 or SKI606 on tyrosine phosphorylation can be overcome when sperm are co-incubated with Ser/Thr phosphatase inhibitors such as okadaic acid (Krapf et al., 2010). Contrary to these findings, inhibition of tyrosine phosphorylation by 10 µM PF431396 was not rescued by okadaic acid, even at concentrations as high as 100 nM (Fig. 1C).

Considering that PF431396 can block both members of the FAK family, we investigated the presence of FAK and PYK2 in sperm extracts by western blotting. Both anti-PYK2 (Fig. 2A) and anti-FAK (Fig. 2B) recognized bands of the expected molecular weight (MW) (~120 kDa) in soluble sperm fractions. Although both antibodies also recognized additional bands at lower MWs, whether or not these bands are related to either PYK2 or FAK has not been established. As PF431396 can block both FAK and PYK2 tyrosine kinases *in vitro* (Fig. 2C, left panel) (Bhattacharya et al., 2012), these results were not sufficient to distinguish which member of the FAK family is involved in sperm tyrosine phosphorylation. To distinguish between PYK2 and FAK, PF573228, a different FAK family inhibitor more selective for FAK than for PYK2, was used (Fig. 2C, right panel). When murine sperm were incubated with PF573228, only a slight decrease in tyrosine phosphorylation was observed in capacitated sperm (Fig. 2D).

The results described above were consistent with the hypothesis that PYK2 was the tyrosine kinase involved in sperm capacitation. However, because many kinase inhibitors are not completely specific, subsequent experiments were carried out using *Pyk2*$^{-/-}$ mice (Okigaki et al., 2003). When sperm from *Pyk2*$^{-/-}$ mice were incubated under capacitating conditions, the increase of protein tyrosine phosphorylation was indistinguishable from that corresponding to wild-type (WT) controls (Fig. 3A). In addition, in WT and *Pyk2*$^{-/-}$ sperm, PF431396 (Fig. 3B) but not PF573228 (Fig. 3C) blocked the capacitation-associated increases of tyrosine phosphorylation. These observations, together with results of western blots using anti-PYK2 and anti-FAK antibodies (Fig. 3D), implied that the normal increase in tyrosine phosphorylation was not due to FAK compensation of the *Pyk2*$^{-/-}$ sperm phenotype. Finally, *Pyk2*$^{-/-}$ mice were fertile (as previously described) (Okigaki et al.,

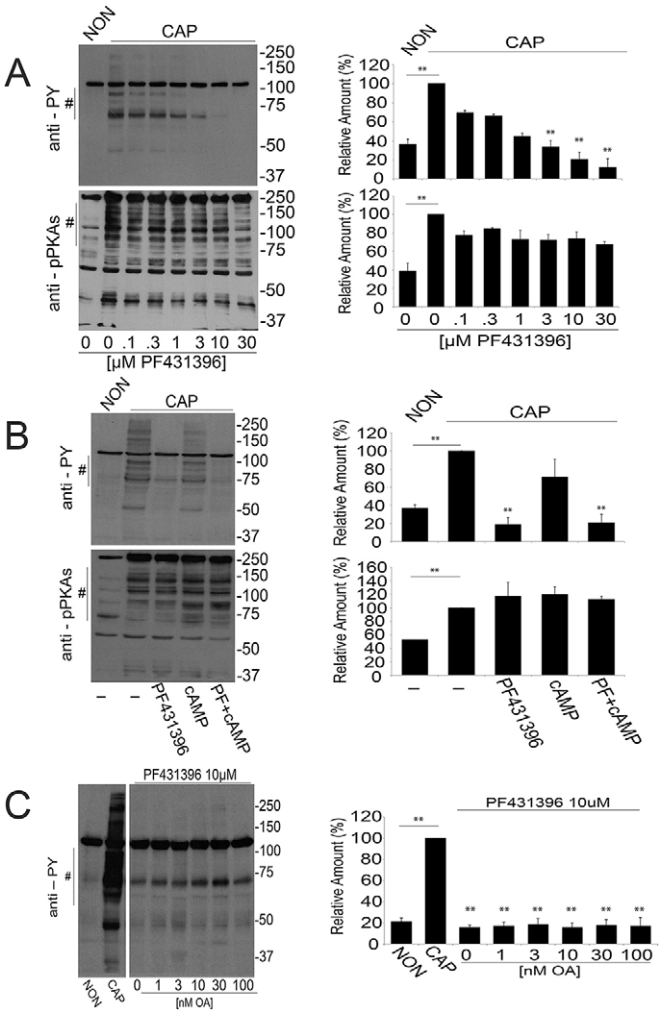

Fig. 1. PF431396 inhibits the capacitation-associated increase in tyrosine phosphorylation. Sperm suspensions (10^6) were diluted in media supplemented (CAP) or not (NON) with $NaHCO_3$ and BSA and in the presence of different compounds as detailed. After 1 h, sperm were analyzed for protein phosphorylation with anti-phosphotyrosine (anti-PY) and anti-phospho PKA substrates (anti-pPKAs). For each experiment (n=3), western blots were analyzed using ImageJ. For comparison between blots, pixels for each lane contained in the region marked by # (proteins in the 70-100 kDa range for PY and 80-200 kDa for pPKAs) were quantified and normalized using the CAP lane as reference (100%). The comparison between groups was performed using two-tailed analysis of variance (ANOVA) in one-way blocks. Multiple comparisons were performed by Tukey's test. Bar graphs represent mean±s.e.m. of the normalized values (**P<0.01). (A) PF431396 concentration curve. Sperm were incubated either in NON or CAP media with increasing concentrations of PF431396, which was added from the beginning of the 60 min incubation. Anti-PY and anti-pPKAs western blot analyses (left panels) and ImageJ quantification (right panels) were conducted. (B) PF431396 blocks cAMP-induced tyrosine phosphorylation. Sperm were incubated either in NON or CAP media in the presence or absence of 1 mM dbcAMP and 100 µM IBMX for 1 h in the presence or in the absence of 10 µM PF431396. Quantification was conducted as described. (C) Okadaic acid (OA) does not overcome inhibition by PF431396. Sperm were incubated for 1 h either in NON or in CAP media in the absence or in the presence of 10 µM PF431396 and in the presence of increasing concentrations of OA. Analyses were carried out as described.

Development (2016) 143, 2325-2333 doi:10.1242/dev.136499

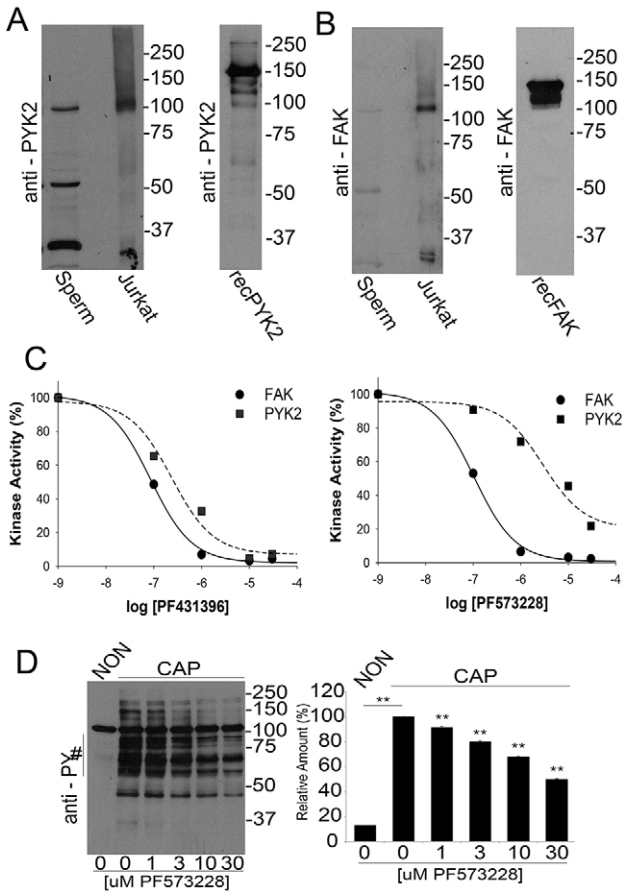

Fig. 2. Presence of FAK subfamily members in sperm and analysis of *in vitro* activity. (A,B) Recombinant proteins (recPYK2, recFAK) or lysates from sperm or Jurkat cells were subjected to western blotting with antibodies for PYK2 (A) or FAK (B). (C) *In vitro* kinase activity of recombinant PYK2 and FAK. Recombinant PYK2 and FAK (60 ng/reaction) were assayed using poly Glu:Tyr as substrate as described. Each of the kinases (tested in triplicate) was assayed in the presence of increasing concentrations of PF431396 (left) and PF573228 (right). Numbers on the *x*-axis are expressed as logarithm of molar concentration. Error bars are in the order of 0.002-0.01 and do not appear in the graph. (D) PF573228 concentration curve. Sperm were incubated for 1 h in NON or in CAP media with increasing concentrations of PF573228. Western blotting using anti-PY antibodies (left) and ImageJ quantification (right) were conducted from independent experiments (n=3). Bars represent the mean± s.e.m. [**P<0.01 versus both CAP (0 µM PF573228) and NON CAP] of the normalized values.

2003) and *in vitro* fertilization success rate was indistinguishable from WT (Fig. 3E).

FER and FERT are responsible for the capacitation-associated increase in tyrosine phosphorylation

The aforementioned results suggest that a PF431396-sensitive tyrosine kinase distinct from FAK and PYK2 is present in mouse sperm and is activated in response to *in vitro* capacitation. Recently, Chung et al. (2014) conducted tyrosine phosphoproteomic analyses in capacitated mouse sperm. A tyrosine phosphopeptide corresponding to the FER activation-loop autophosphorylation site was among the unique phosphopeptides identified. In addition to the ubiquitously expressed FER, it is known that testicular germ cells express a testis-specific splicing variant known as FERT (Fischman et al., 1990; Kierszenbaum et al., 2008). Consistently, antibodies against FER detected one band in murine spermatozoa at ∼50 kDa, corresponding to the predicted MW of FERT (Fig. 4A). However, in some experiments, a second protein with a MW of ∼100 kDa (the predicted MW of somatic FER) was also observed (e.g. Fig. 4F). Moreover, recombinant FER was sensitive to PF431396 *in vitro* with an IC_{50} of ∼1 µM (Fig. 4B) suggesting that this tyrosine kinase could be the PF431396 target in sperm. Considering that most of the substrates phosphorylated on tyrosine found in capacitated sperm are insoluble in non-ionic detergents such as Triton X-100 (Fig. 4C), the solubility of FERT, PYK2 and FAK was analyzed. Whereas PYK2 (Fig. 4D) and FAK (Fig. 4E) were mostly present in the Triton X-100-soluble fractions, FERT (Fig. 4F) was found in both the soluble and insoluble fractions. Interestingly, most of the soluble FERT exhibited an increased apparent MW, suggesting that FERT is post-translationally modified during solubilization.

To explore further the involvement of FER in sperm tyrosine phosphorylation pathways, we employed mice targeted with a kinase-inactivating (D743R) mutation in *Fer* (Craig et al., 2001) ($Fer^{DR/DR}$). Sperm from $Fer^{DR/DR}$ mice did not display increased tyrosine phosphorylation when incubated under conditions that support capacitation (Fig. 5B, upper panel). Additionally, phosphorylation of PKA substrates was not affected (Fig. 5B, lower panel). $Fer^{DR/DR}$ mice are fertile *in vivo* (Craig et al., 2001); however, sperm from these mice almost completely failed to fertilize metaphase II eggs *in vitro* (Fig. 5C). Other sperm parameters, such as morphology, spontaneous and ionophore-induced acrosome reaction, percentage of motile cells and hyperactivation, were similar in WT, $Pyk2^{-/-}$ and $Fer^{DR/DR}$ sperm (Fig. S1).

The localization of proteins phosphorylated on tyrosine residues has been accurately measured in three dimensions (3D) using stochastic optical reconstruction microscopy (STORM), a super-resolution imaging technique (Chung et al., 2014). STORM measurements indicated that in the principal piece, tyrosine phosphorylation is confined to the axoneme of the sperm flagellum. Here, we used 3D STORM to evaluate the spatial distribution of FER within the sperm flagellum. FER was found throughout both the midpiece and principal piece (Fig. 6A). Cross-sections of the images indicated that in the midpiece, FER localized within 250 nm from the center (Fig. 6B). In the principal piece, FER had a spatial distribution restricted to the axoneme (Fig. 6C). A similar spatial distribution was observed for tyrosine phosphorylation in both sections of the flagellum (Fig. 6D-F). The coincident radius in the radial distributions of both signals shows that FER localization overlaps with the localization of tyrosine phosphorylation in both compartments of the sperm flagellum (Fig. 6G,H). Consistent with immunofluorescence data for FER and phosphotyrosine (Fig. S2A,B), no signal was detected during the analysis of sperm heads by STORM. Probably owing to instability of the $FER^{DR/DR}$ protein, FER (and FERT) is lost from sperm from $Fer^{DR/DR}$ mice (Fig. S2B,C).

DISCUSSION

During maturation in the epididymis, sperm acquire progressive motility; however, they cannot fertilize until they reside in the female tract for a period of time. The independent discovery of capacitation by Chang (1951) and Austin (1951) set the stage for development of *in vitro* fertilization techniques. Capacitation can be mimicked *in vitro* in defined media (Buffone et al., 2014). At the molecular level, capacitation is associated with sequential activation of different signaling pathways including: (1) fast activation of

Development (2016) 143, 2325-2333 doi:10.1242/dev.136499

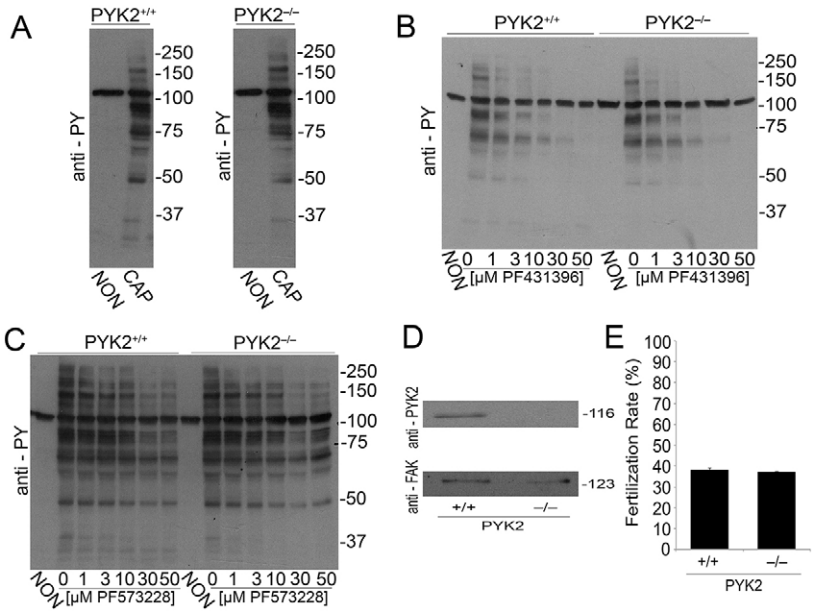

Fig. 3. Sperm from *Pyk2*$^{-/-}$ mice undergo normal tyrosine phosphorylation. (A) Tyrosine phosphorylation analysis. Sperm from either wild-type (*Pyk2*$^{+/+}$) or knockout (*Pyk2*$^{-/-}$) mice were incubated either under NON or CAP conditions. After 1 h incubation, tyrosine phosphorylation was assessed by anti-PY western blotting. Images are representative of three independent experiments (*n*=3) using three different animals. (B,C) PF431396 and PF573228 concentration curves. The effect of PF431396 (B) and of PF573228 (C) on tyrosine phosphorylation was analyzed as described for Fig. 1A. (D) Anti-PYK2 and anti-FAK western blot analyses of *Pyk2*$^{+/+}$ and *Pyk2*$^{-/-}$ sperm. Cauda epididymal sperm from either *Pyk2*$^{+/+}$ or *Pyk2*$^{-/-}$ mice were obtained in TYH-HEPES media as described above, and sperm cell lysates prepared. The presence of PYK2 and FAK was analyzed by independent western blotting run in parallel. (E) Sperm from *Pyk2*$^{-/-}$ animals are fertile *in vitro*. Cauda epididymal sperm from either *Pyk2*$^{+/+}$ or *Pyk2*$^{-/-}$ mice were collected in TYH media as described in Materials and Methods and capacitated for 1 h, and rates of *in vitro* fertilization (IVF) evaluated as described in Materials and Methods. Bar graphs represent the mean± s.e.m. of the normalized values of three independent experimental replicates (*n*=3), using three different animals. IVF data were analyzed by the simple χ^2 test.

cAMP synthesis (Visconti, 2009); (2) increase in intracellular pH (pHi) (Parrish et al., 1989; Zeng et al., 1996); (3) hyperpolarization of the plasma membrane (Escoffier et al., 2012; Zeng et al., 1995); (4) increase in intracellular Ca^{2+} (Baldi et al., 1991; Carlson et al., 2007; Marin-Briggiler et al., 2003); and (5) increase in tyrosine phosphorylation (Visconti et al., 1995a). Our group has shown that the increase in tyrosine phosphorylation is downstream of the activation of a cAMP-dependent pathway (Visconti et al., 1995a,b). However, the identity of the tyrosine kinase responsible for this activation has remained elusive over the years.

In two subsequent papers, Baker and colleagues (Baker et al., 2006; Mitchell et al., 2008) proposed SRC as the tyrosine kinase responsible for the increase in tyrosine phosphorylation observed during capacitation. These authors detected activation of SRC by mass spectrometry during capacitation, and also showed that inhibitors of SRC were able to block the capacitation-associated increase in tyrosine phosphorylation. More recently, our group has confirmed these observations (Krapf et al., 2010). However, we showed that SRC inhibitors were capable of blocking the early phosphorylation of PKA substrates as well. This inhibition of phosphorylation pathways was overcome by co-incubation with either okadaic acid or calyculin A, two very specific inhibitors of Ser/Thr phosphatases (Krapf et al., 2010). Moreover, although sperm from *Src*$^{-/-}$ mice were infertile and unable to fertilize oocytes *in vitro*, they displayed normal increases in tyrosine phosphorylation. Altogether, these results suggested that although SRC and/or SRC kinase family members have essential roles in the regulation of sperm function, SRC was not the tyrosine kinase involved in the regulation of the increase in tyrosine phosphorylation associated with capacitation.

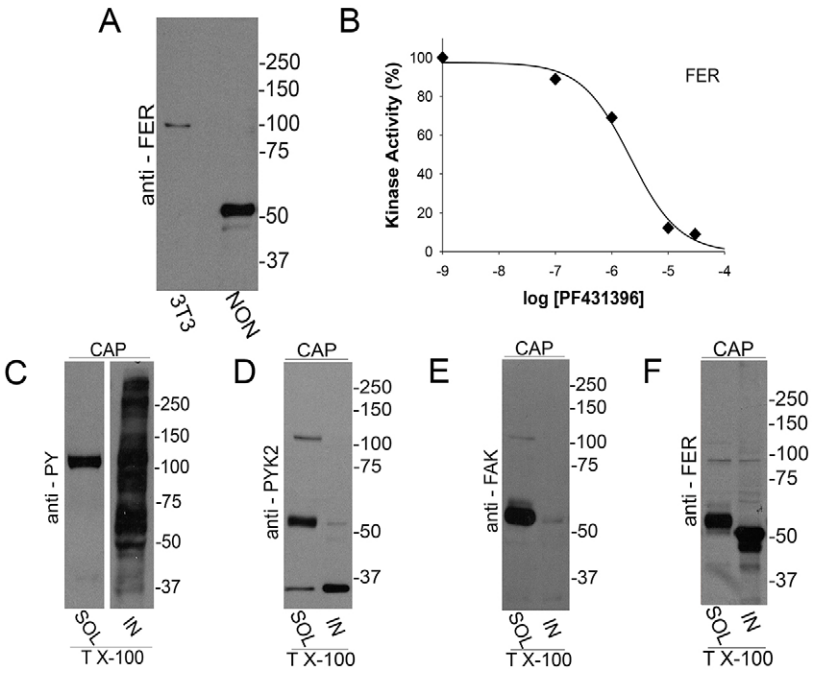

Fig. 4. Presence of FER in mouse sperm. (A) Presence of FERT in mouse sperm. Sperm (or NIH3T3 cell lysates for control) were analyzed by western blotting using anti-FER antibodies. (B) FER *in vitro* kinase assay. Recombinant FER (60 ng) *in vitro* kinase activity was assayed as described for PYK2 and FAK in Fig. 2C. Values represent mean±s.e.m. (*n*=3). Error bars are in the order of 0.01-0.08 and do not appear in the graph. (C-F) Distribution of PYK2, FAK, FER and PY substrates after solubilization with Triton X-100 (1%). Cauda epididymal sperm obtained as described in Fig. 1 were incubated in conditions that support capacitation for 1 h. Sperm were then washed in PBS, and Triton X-100-treated samples prepared as described in Materials and Methods. Triton X-100-soluble (SOL) and insoluble (IN) fractions were separated, boiled in SDS-sample buffer for 5 min and analyzed by western blotting using anti-PY (C), anti -PYK2 (D), anti -FAK (E) and anti -FER (F). Results are representative of three independent experiments (*n*=3) using different animals.

Development (2016) 143, 2325-2333 doi:10.1242/dev.136499

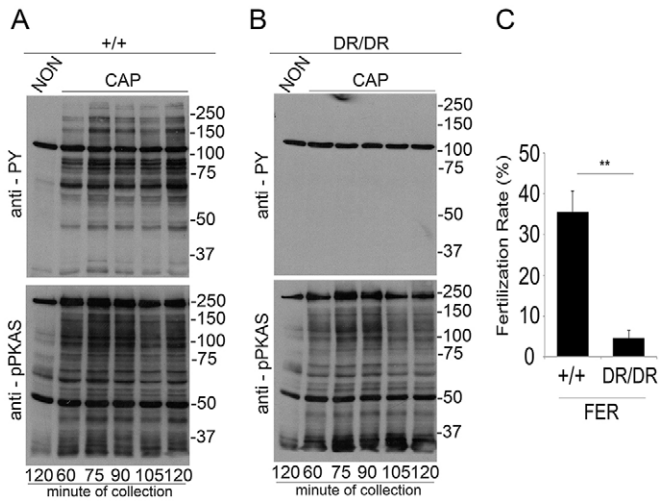

Fig. 5. Sperm from *Fer*$^{DR/DR}$ mice do not display capacitation-associated increases in tyrosine phosphorylation. (A,B) Sperm from either wild-type (+/+) (A) or *Fer*$^{DR/DR}$ (DR/DR) mice (B) were obtained as described for Fig. 1 and incubated under NON or CAP conditions. Time-dependent response by phosphorylation of PKA substrates and by tyrosine phosphorylation was assessed using anti-PY (upper panels) and anti-pPKAs (lower panels) by western blotting. Images shown are representative of at least three independent experiments (n=3). (C) Sperm from *Fer*$^{DR/DR}$ mice are subfertile *in vitro*. Cauda epididymal sperm from either wild-type (+/+) or *Fer*$^{DR/DR}$ (DR/DR) mice were obtained in TYH media and capacitated for 1 h, and IVF rates were evaluated as described in Materials and Methods. Bar graphs represent the mean±s.e.m. of the normalized values (**P<0.01) (n=3). IVF data were analyzed by the simple χ^2 test.

In 2013, Gonzalez-Fernandez et al. presented evidence suggesting that kinases belonging to the FAK family were responsible for the capacitation-associated increase of tyrosine phosphorylation in stallion sperm (Gonzalez-Fernandez et al., 2013). Similar to the case of SRC, this evidence was obtained using antibodies recognizing active members of PYK2 and FAK, and commercial inhibitors against this kinase family. Using a similar approach, our group has recently proposed PYK2 as the kinase responsible for tyrosine phosphorylation in human spermatozoa (Battistone et al., 2014). Interestingly, contrary to SRC blockers, results of this study showed that the FAK kinases inhibitor PF431396 blocked tyrosine phosphorylation without inhibiting phosphorylation of PKA substrates. Altogether, these findings suggested a role for FAK family members in the capacitation-induced increase in tyrosine phosphorylation. However, this hypothesis was based on the use of kinase inhibitors, which might have off-target effects. To avoid this problem, we have used a combination of pharmacological and genetic approaches in this study. Similar to observations in stallion and human sperm, the FAK/PYK2 inhibitor PF431396 blocked the increase in tyrosine phosphorylation without affecting PKA activation. The more specific FAK inhibitor PF573228 was significantly less effective at blocking tyrosine phosphorylation in mouse sperm, suggesting that FAK was not involved in this signaling event. Although these results supported PYK2 as the tyrosine kinase involved in capacitation, sperm from *Pyk2*$^{-/-}$ mice were fertile and exhibited normal capacitation-induced tyrosine phosphorylation. The increase in tyrosine phosphorylation in these sperm was blocked with PF431396, but not with PF573228, suggesting that the absence of PYK2 was not compensated by increased levels of FAK. In addition, these data indicated that another tyrosine kinase sensitive to PF431396 was responsible for the capacitation-associated increase of tyrosine phosphorylation in mouse sperm.

Recent tandem mass spectrometry data has shown that the protein kinase FER is present in mature mouse sperm and undergoes tyrosine phosphorylation in its kinase domain during capacitation (Chung et al., 2014). FER is a non-receptor tyrosine kinase closely related structurally to the proto-oncogene *Fes* (feline sarcoma oncogene; also known as *Fps*, Fujinami poultry sarcoma) (Greer, 2002). These kinases have been implicated in the regulation of cell-cell and cell-matrix interactions. In this work, we show that anti-FER antibodies recognize two bands by western blot in sperm extracts; this result is consistent with the presence of the two known mRNA splicing variants of *Fer* in testicular germ cells, which are translated into the ubiquitously expressed p94-FER and the shorter testis-specific p51-FERT. Both isoforms contain functional kinase domains. In addition to its presence in sperm, *in vitro* kinase activity experiments using recombinant FER demonstrated that this tyrosine

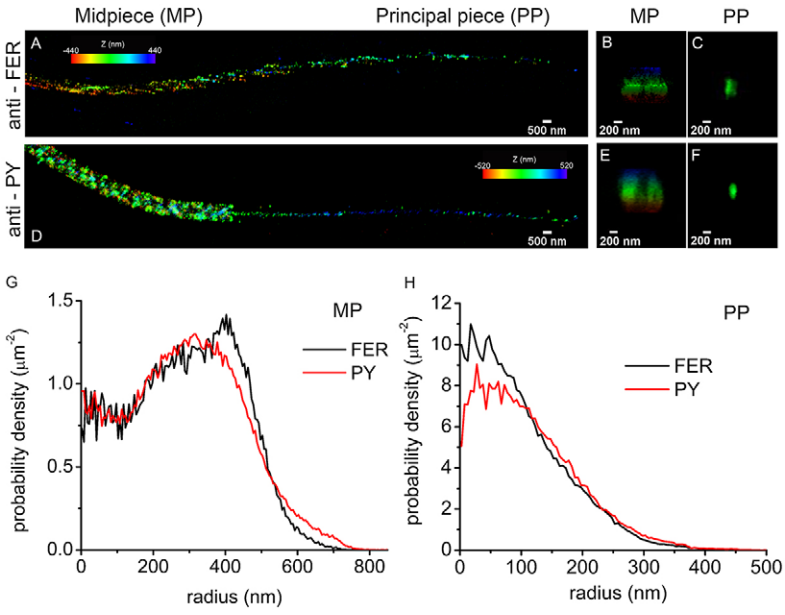

Fig. 6. Localization of FER and tyrosine-phosphorylated proteins in mouse sperm by STORM. (A) 3D STORM images of FER in *xy* projection. The color represents the relative distance from the focal plane along the *z*-axis. (B) FER localization in the midpiece (MP), *yz* projection. (C) FER localization in the principal piece (PP), *yz* projection. (D) 3D STORM images of tyrosine phosphorylation (pY) in *xy* projection. The color represents the relative distance from the focal plane along the *z*-axis. (E) Tyrosine-phosphorylated protein (PY) localization in the MP, *yz* projection. (F) Tyrosine-phosphorylated protein (PY) localization in the PP, *yz* projection. (G) Radial distribution of FER and PY in the MP. (H) Radial distribution of FER and PY in the PP. Images are representative of 15 cells from three different animals for PY analysis and of nine cells from three different animals for FER analysis.

Development (2016) 143, 2325-2333 doi:10.1242/dev.136499

kinase is sensitive to PF431396. Moreover, the IC_{50} for *in vitro* kinase inhibition and the EC_{50} for inhibition of tyrosine phosphorylation in capacitated sperm were in the same concentration range.

FER function has been explored *in vivo* using a mouse model in which the endogenous *Fer* locus is targeted with a missense mutation (Craig et al., 2001). In the resulting D743R mutant, FER and FERT proteins lack kinase activity, and the protein is unstable. $Fer^{DR/DR}$ mice show several defects, which implicate FER in growth factor signaling (Craig et al., 2001), hematopoiesis (Senis et al., 2003), tumorigenesis (Sangrar et al., 2015), regulation of the cytoskeleton (Sangrar et al., 2007; Xu et al., 2004) and inflammatory cell functions (Craig and Greer, 2002; Khajah et al., 2013; McCafferty et al., 2002). Here, we used this murine model to evaluate the role of FER and FERT in the capacitation-associated increase of tyrosine phosphorylation. Our results showed that in sperm from $Fer^{DR/DR}$ animals, the initial PKA activation was not affected. However, the increase in tyrosine phosphorylation was obliterated. Interestingly, hexokinase type I remained phosphorylated in tyrosine residues (Kalab et al., 1994) indicating that tyrosine phosphorylation of this enzyme is not dependent on FER. Altogether, these results indicate that FERT (or FER) is responsible for the increase in tyrosine phosphorylation observed in murine sperm during capacitation. Consistently, 3D-STORM microscopy using anti-phosphotyrosine and anti-FER antibodies showed coincident spatial distributions in both mid- and principal piece in capacitated sperm flagella.

In the last 20 years, tyrosine phosphorylation has been used as a marker of capacitation in sperm from mouse and other species. Capacitation is defined as all biochemical and physiological processes that render the sperm able to fertilize (Yanagimachi, 1994). As $Fer^{DR/DR}$ mice are viable and fertile (Craig et al., 2001), our findings suggest that, at least in mouse sperm, the capacitation-associated increase in tyrosine phosphorylation is not required for *in vivo* fertilization. However, our *in vitro* results do not exclude the possibility that during natural mating, interactions between sperm and the female environment compensate for the lack of FER. Despite these results, $Fer^{DR/DR}$ sperm are less able to fertilize *in vitro*. Interestingly, mice lacking cysteine-rich secretory protein 1 (CRISP1) exhibited a similar phenotype. CRISP1 is expressed by the epididymal epithelium, secreted and incorporated into sperm during epididymal maturation (Da Ros et al., 2015). Although these mice are fertile *in vivo*, their capacitated sperm have significantly lower levels of tyrosine phosphorylation *in vitro* (Da Ros et al., 2008). Both $Crisp1^{-/-}$ and $Fer^{DR/DR}$ sperm exhibit reduced *in vitro* fertilization rates, suggesting that the functional role of tyrosine phosphorylation *in vivo* can be bypassed by yet undiscovered mechanisms. The finding that tyrosine phosphorylation plays a role in *in vitro* fertilization, together with results showing that the increase in tyrosine phosphorylation during capacitation is conserved in a variety of mammalian species, suggests that this signaling pathway could play a role in species in which sperm competition is relevant. However, direct evaluation of this hypothesis requires further investigation.

MATERIALS AND METHODS

Materials

Reagents were purchased from various sources. Sodium bicarbonate ($NaHCO_3$), bovine serum albumin (BSA, fatty acid free), dibutyryl cAMP (Bt_2cAMP), 3-isobutyl-1-methylxanthine (IBMX), adenosine triphosphate (ATP), magnesium chloride ($MgCl_2$), manganese chloride ($MnCl_2$), aprotinin, leupeptin, sodium orthovanadate ($NaVO_4$), *p*-nitrophenyl phosphate (NPP), β-glycero phosphate (βGP), β-mercaptoethanol, poly (Glu:Tyr)(1:4) and PF431396 were obtained from Sigma-Aldrich. SU6656 was purchased from Cayman Chemical (Ann Harbor, MI, USA), okadaic acid was provided by LC Laboratories (Woburn, MA, USA). PF573228 was obtained from Selleck Biochem (Houston, TX, USA). HEPES was purchased from Roche and paraformaldehyde from Electron Microscopy Science (Hatfield, PA, USA). Radiolabeled adenosine triphosphate (γ^{32}P-ATP) was purchased from Perkin Elmer. Rabbit monoclonal anti-phospho-PKA substrates (clone 100G7E, lot #18, anti-pPKAs) (Navarrete et al., 2015), mouse monoclonal anti-total PYK2 (clone 5E2, lot #1) (Tang et al., 2002), rabbit polyclonal anti-FAK (cat# 3285, ot #9) (Battistone et al., 2014) and mouse monoclonal anti-FER (cat#4268, lot #2) (Greer, 2002) were purchased from Cell Signaling Technology. Mouse monoclonal anti-phospho tyrosine (anti-PY) antibody (clone 4G10, lot #2658756) (Navarrete et al., 2015) was obtained from EMD Millipore. Peroxidase/conjugated anti-mouse IgG were obtained from Jackson ImmunoResearch and peroxidase-conjugated anti-rabbit IgG from GE Healthcare. Alexa Fluor 647-conjugated anti-mouse secondary antibody was purchased from Invitrogen (ThermoFisher Scientific). His-Tag recombinant PYK2, FAK and FER were purchased from Invitrogen.

Sample preparation

Animals were euthanized in accordance with the Institutional Animal Care and Use Committee (IACUC) guidelines of University of Massachusetts. Cauda spermatozoa were collected from CD1 retired breeders (Charles River Laboratories, Wilmington, MA, USA) from young adult C57 (7- to 8-week-old mice), $Pyk2^{-/-}$ (Shen et al., 2011), $Fer^{DR/DR}$ (Craig et al., 2001) mice and their respective wild-type controls. Each cauda epididymis was placed in 500 µl of a modified Krebs-Ringer medium (TYH/HEPES) (Kito and Ohta, 2008). This medium does not support mouse sperm capacitation. After 10 min incubation at 37°C (swim-out), epididymis tissue debris was removed, and the suspension adjusted to a final concentration of $1\text{-}2\times10^7$ cells/ml. The sperm were then incubated at 37°C for the times indicated in each experiment, in the absence (NON) or in the presence (CAP) of 15 mM $NaHCO_3$ and 5 mg/ml BSA. To test the effect of inhibitors, sperm were incubated under the conditions described above in the presence of increasing concentrations of inhibitors as indicated. These compounds were assayed for 1 h and were added from the beginning of the incubation period. For *in vitro* fertilization (IVF) assays, sperm were first incubated in modified TYH medium (without HEPES) containing 25 mM $NaHCO_3$ and 5 mg/ml BSA. The medium was previously equilibrated in a humidified atmosphere of 5% CO_2 at 37°C (Wertheimer et al., 2008).

SDS-PAGE and immunoblotting

Sperm were collected by centrifugation, washed in 1 ml of PBS, re-suspended in Laemmli sample buffer (Laemmli, 1970), boiled (5 min) and centrifuged at 12,100 ***g***. Supernatants were then supplemented with 5% β-mercaptoethanol and boiled (3 min). Protein extracts were analyzed by SDS-PAGE and electro-transferred to PVDF (Bio-Rad). Immunoblotting was conducted with the appropriate antibodies: anti-pPKAs (clone 100G7E); anti-PY (clone 4G10); anti-FAK; anti PYK2 (5D2) and anti-FER (5E2). PVDF membranes were blocked with 5% fish gelatin (for anti-phosphoantibodies) and 5% fat-free milk in TBS containing 0.1% Tween 20 (T-TBS) (for all the others) and antibodies used at a final concentration of 1:1000. Secondary antibodies were diluted in T-TBS (1:10,000). Enhanced chemioluminescence ECL Plus Kit (GE Healthcare) was used for detection. Tyrosine phosphorylated hexokinase served as a loading control (Porambo et al., 2012; Visconti et al., 1995a). When necessary, PVDF membranes were stripped at 65°C for 20 min in 2% SDS, 0.74% β-mercaptoethanol, 62.5 mM Tris, pH 6.5, and then washed six times for 5 min each in T-TBS prior to re-probing. Image analysis was conducted using ImageJ (http://imagej.nih.gov/ij). Western blotting regions of interest (ROIs) used for quantification are indicated by a vertical bar on the left of the respective graph. In all cases, results were normalized arbitrarily considering the CAP lane as the unit value. Images shown are representative of experiments repeated three times (n=3) using three different animals.

Development (2016) 143, 2325-2333 doi:10.1242/dev.136499

Recombinant kinase assay

Sixty nanograms of each GST-tagged recombinant kinase (PYK2, FAK and FER) were assayed in a buffer containing: 25 mM HEPES (pH 7.2), 10 mM $MgCl_2$, 10 mM $MnCl_2$, 10 µM aprotinin, 10 µM leupeptin, 100 µM $NaVO_4$, 5 mM nitrophenyl phosphate (NPP), and 40 mM β-glycero phosphate (βGP), with 40 µM ATP and 100 µM poly(Glu:Tyr) (1:4) as substrate for 20 min in the presence of 1 µCi of γ^{32}P-ATP. Reactions were stopped by adding 60% trichloric acid (final concentration 30%), cooling on ice for 20 min and centrifuging for 3 min at 10,000 ***g***. Thirty microliters (30 µl) of the supernatant were transferred to phosphocellulose paper (Whatman P81, Millipore; 2 cm×2 cm). Papers were immersed in 5 mM phosphoric acid and washed seven times with the same solution. At the end of the washes, spotted papers were rinsed with ethanol and air-dried. Counts (cpm) incorporated were evaluated in vials with 2.5 ml of scintillation fluid in a Beckman counter LS6500. Values represent average of three independent experimental replicates (n=3).

Mouse eggs collection and IVF assays

Metaphase II-arrested eggs were collected from 6- to 8-week-old, super-ovulated C57BL/6 female mice (Charles River Laboratories) at 12 h after human chorionic gonadotropin intraperitoneal injection (Wertheimer et al., 2008). The cumulus-oocyte complexes were placed into a well with 500 µl of TYH (without HEPES) media previously equilibrated in an incubator with 5% CO_2 at 37°C. Fertilization wells containing 25-40 eggs were inseminated with sperm (final concentration of 2.5×10^5 cells/ml) that had been incubated for 1 h and 20 min in TYH medium supporting capacitation. After 4 h of insemination, eggs were washed, moved into fresh TYH media, and evaluated 24 h post-insemination. Two-cell-stage embryos were assigned as fertilized. Values represent average of three independent experimental replicates (n=3), using three different animals.

Analysis of solubility

The solubility of tyrosine kinases (PYK2, FAK and FER) under investigation in sperm was assessed using 1% Triton X-100 after incubation in media that support capacitation. Briefly, after 1 h incubation, sperm were centrifuged at 1500 rpm (150 ***g***) for 5 min and re-suspended in 1% Triton X-100/PBS buffer containing protease and phosphatase inhibitors. Cell lysis proceeded by incubation on ice for 30 min. Samples were then spun down at 14,000 rpm (17,500 ***g***) at 4°C for 2 min, and both supernatant (Triton X-100-soluble fraction) as well as the remaining pellets (Triton X-100-insoluble fraction) were analyzed by western blotting. Images are representative of experiments repeated three times (n=3).

Genotyping of *Pyk2*$^{-/-}$ and *Fer*$^{DR/DR}$

Genotyping of *Pyk2*$^{-/-}$ was performed as previously described (Shen et al., 2011) using the following primers: *Pyk2* wild type forward, 5′-GGAGG-TCTATGAAGGTGTCTACACGAAC-3′; *Pyk2* mutant forward, 5′-GCC-AGCTCATTCCTCCCACTCAT-3′; *Pyk2* reverse, 5′-CCTGCTGGCAG-CCTAACCACAT-3′. Genotyping of *Fer*$^{DR/DR}$ was evaluated following the protocol by Craig et al. (2001).

Immunofluorescence and super-resolution microscopy

After capacitation, sperm were centrifuged at 800 ***g*** for 5 min, the pellet was fixed in 4% paraformaldehyde for 10 min at room temperature (RT) and then centrifuged at 800 ***g*** for 5 min. The pellet was re-suspended in PBS and 50 µl of this suspension were placed onto polylysine-coated coverslips for 10 min. Bound cells were permeabilized with 0.5% Triton X-100 in PBS for 5 min and blocked with 3% BSA in PBS for 1 h (RT). Primary antibodies were diluted in 1% BSA, and incubated with cells overnight at 4°C in a humidified chamber. Anti-PY antibody (clone 4G10; final concentration 1:1000), and anti-FER (clone 5D2) at a dilution of 1:50 were used. After primary antibody incubation, cells were washed with T-PBS (0.5% Tween-20 in PBS) three times for 5 min each, and then stained with Alexa Fluor 647-conjugated anti-mouse secondary antibody diluted in PBS containing 1% BSA (1:1000 for pY and 1:500 for FER) at RT for 1 h. Cells were then washed with T-PBS three times for 5 min each and for STORM analysis incubated with 50 nm gold nanoparticles (Nanopartz, Loveland, CO, USA) that were used as fiducial markers for drift correction (only for STORM). After washing, cells were immediately mounted. Imaging buffer for both standard immunofluorescence and STORM was 50 mM Tris-HCl (pH 8.0), 10 mM NaCl, 10% glucose, 0.56 mg/ml glucose oxidase, 34 µg/ml catalase, 10% glucose and 1% β-mercaptoethanol.

STORM imaging

Image stacks were acquired using Andor IQ 2.3 software in a custom-built microscope equipped with an Olympus PlanApo 100×/1.45 objective (Weigel et al., 2011). Alexa Fluor 647 was excited with a 638 nm laser (DL638-050, CrystaLaser, Reno, NV, USA) under continuous illumination. Initially, the photo-switching rate was sufficient to provide a substantial fluorophore density. However, as fluorophores photo-bleached, a 405 nm laser was introduced to accelerate the photo-switching rate. The intensity of the 405 nm laser was adjusted to control the density of active fluorophores. A cylindrical lens with a focal length of 1 m was placed in the detection path in order to achieve 3D resolution as previously described (Huang et al., 2008). The images were acquired in a back-illuminated electron-multiplied charge-coupled device (EMCCD) camera (Andor iXon DU-888) operated at −85°C at a rate of 23 frames/s. Fifty-thousand frames were collected to generate a super-resolution image.

Super-resolution image reconstruction and analysis

Single-molecule localization, drift correction using gold fiducial markers and reconstruction were performed with ThunderSTORM, an ImageJ plugin (Ovesny et al., 2014). In order to find the molecular radial distributions, we selected regions of interest of the flagellum that were found to lie in a straight line, and the center of the flagellar cross-section was calculated in MATLAB with a custom-written algorithm. The coordinates of the localized molecules were then transformed into cylindrical coordinates (Chung et al., 2014), from which the distribution of radial localization was computed.

Motility and acrosome reaction assays

Motility parameters were analyzed in capacitated sperm from the different transgenic models using Hamilton-Thorne CASA system (Beverly, MA, USA) and CASAnova software as described (Goodson et al., 2011). Spontaneous and A23187 (10 µM)-induced acrosome reaction was measured as described (Wertheimer et al., 2008) in sperm from WT, *Pyk2*$^{-/-}$ and *Fer*$^{DR/DR}$ mice. Briefly, capacitated sperm were incubated with Ca^{2+} ionophore A23187 or DMSO (control) for 30 min, and then stained with PNA-Alexa 488 (Molecular Probes, L-21409). The number of sperm with or without acrosome was counted under a fluorescence microscope. Data are expressed as percentage of reacted sperm.

Statistics

Statistical analyses were performed using the software Infostat 2011 (www.infostat.com.ar). All data were verified to accomplish the parametric assumptions: homogeneity of variances and normality. For western blotting experiments, experiments were repeated at least three times and comparison between groups was performed by analysis of variance (ANOVA) in blocks. Data from each western analysis was considered as a block and all treatments were applied to it. When the ANOVA tests were significantly different between groups (P<0.05), multiple comparisons were performed by Tukey's test. For the IVF experiments, data was analyzed by χ^2 test. P-values (P<0.001, P<0.01 or P<0.05) were considered to be significant as indicated in the figure legends.

Acknowledgements

The *Pyk2*$^{-/-}$ mice, originally developed by Dr Charles Turner from Purdue University, were obtained from Dr Assoian's lab (Department of Systems Pharmacology and Translational Therapeutics, University of Pennsylvania).

Competing interests

The authors declare no competing or financial interests.

Author contributions

A.A. and M.A.B. conducted experiments; P.E.V., P.C., A.D., D.K., V.G.D.R. and A.A. designed experiments, analyzed data, discussed findings and prepared the manuscript; C.S.-C. and J.L.D.I.V.-B. discussed results; A.A. and F.A.N. performed IVF and CASA analyses; M.G.G. performed indirect immunofluorescence; M.G.G. and X.X. performed STORM; A.M.S. helped with experimental design and animal protocols, discussed findings and corrected the manuscript; P.G. donated $Fer^{DR/DR}$ animals. All authors contributed specific parts of the manuscript, with P.E.V., and A.A. assuming responsibility for the manuscript in its entirety.

Funding

This study was supported by the Eunice Kennedy Shriver National Institute of Child Health and Human Development NIH [RO1 HD38082 and HD44044 to P.E.V.]; the Canadian Institutes of Health Research (P.A.G.); the National Science Foundation [1401432 to D.K.]; the Consejo Nacional de Ciencia y Tecnología CONACyT-Mexico 49113 and Dirección General Asuntos del Personal Académico, Universidad Nacional Autónoma de México (DGAPA/UNAM) [IN202312] to A.D.; and the National Scientific and Technical Research Council (CONICET) [PIP 2012-2014 No 905 to P.S.C.]. Deposited in PMC for release after 12 months.

Supplementary information

Supplementary information available online at
http://dev.biologists.org/lookup/doi/10.1242/dev.136499.supplemental

References

Austin, C. R. (1951). Observations on the penetration of the sperm in the mammalian egg. *Aust. J. Sci. Res. Ser. B Biol. Sci.* **4**, 581-596.

Baker, M. A., Hetherington, L. and Aitken, R. J. (2006). Identification of SRC as a key PKA-stimulated tyrosine kinase involved in the capacitation-associated hyperactivation of murine spermatozoa. *J. Cell Sci.* **119**, 3182-3192.

Baker, M. A., Hetherington, L., Curry, B. and Aitken, R. J. (2009). Phosphorylation and consequent stimulation of the tyrosine kinase c-Abl by PKA in mouse spermatozoa; its implications during capacitation. *Dev. Biol.* **333**, 57-66.

Baldi, E., Casano, R., Falsetti, C., Krausz, C., Maggi, M. and Forti, G. (1991). Intracellular calcium accumulation and responsiveness to progesterone in capacitating human spermatozoa. *J. Androl.* **12**, 323-330.

Baldi, E., Luconi, M., Bonaccorsi, L. and Forti, G. (2002). Signal transduction pathways in human spermatozoa. *J. Reprod. Immunol.* **53**, 121-131.

Battistone, M. A., Alvau, A., Salicioni, A. M., Visconti, P. E., Da Ros, V. G. and Cuasnicu, P. S. (2014). Evidence for the involvement of proline-rich tyrosine kinase 2 in tyrosine phosphorylation downstream of protein kinase A activation during human sperm capacitation. *Mol. Hum. Reprod.* **20**, 1054-1066.

Bhattacharya, S. K., Aspnes, G. E., Bagley, S. W., Boehm, M., Brosius, A. D., Buckbinder, L., Chang, J. S., Dibrino, J., Eng, H., Frederick, K. S. et al. (2012). Identification of novel series of pyrazole and indole-urea based DFG-out PYK2 inhibitors. *Bioorg. Med. Chem. Lett.* **22**, 7523-7529.

Buck, J., Sinclair, M. L., Schapal, L., Cann, M. J. and Levin, L. R. (1999). Cytosolic adenylyl cyclase defines a unique signaling molecule in mammals. *Proc. Natl. Acad. Sci. USA* **96**, 79-84.

Buffone, M. G., Wertheimer, E. V., Visconti, P. E. and Krapf, D. (2014). Central role of soluble adenylyl cyclase and cAMP in sperm physiology. *Biochim. Biophys. Acta* **1842**, 2610-2620.

Carlson, A. E., Hille, B. and Babcock, D. F. (2007). External Ca2+ acts upstream of adenylyl cyclase SACY in the bicarbonate signaled activation of sperm motility. *Dev. Biol.* **312**, 183-192.

Chang, M. C. (1951). Fertilizing capacity of spermatozoa deposited into the fallopian tubes. *Nature* **168**, 697-698.

Chung, J.-J., Shim, S.-H., Everley, R. A., Gygi, S. P., Zhuang, X. and Clapham, D. E. (2014). Structurally distinct Ca(2+) signaling domains of sperm flagella orchestrate tyrosine phosphorylation and motility. *Cell* **157**, 808-822.

Craig, A. W. B. and Greer, P. A. (2002). Fer kinase is required for sustained p38 kinase activation and maximal chemotaxis of activated mast cells. *Mol. Cell. Biol.* **22**, 6363-6374.

Craig, A. W. B., Zirngibl, R., Williams, K., Cole, L.-A. and Greer, P. A. (2001). Mice devoid of fer protein-tyrosine kinase activity are viable and fertile but display reduced cortactin phosphorylation. *Mol. Cell. Biol.* **21**, 603-613.

Da Ros, V. G., Maldera, J. A., Willis, W. D., Cohen, D. J., Goulding, E. H., Gelman, D. M., Rubinstein, M., Eddy, E. M. and Cuasnicu, P. S. (2008). Impaired sperm fertilizing ability in mice lacking Cysteine-RIch Secretory Protein 1 (CRISP1). *Dev. Biol.* **320**, 12-18.

Da Ros, V. G., Munoz, M. W., Battistone, M. A., Brukman, N. G., Carvajal, G., Curci, L., Gomez-Ellas, M. D., Cohen, D. B. and Cuasnicu, P. S. (2015). From the epididymis to the egg: participation of CRISP proteins in mammalian fertilization. *Asian J. Androl.* **17**, 711-715.

Escoffier, J., Krapf, D., Navarrete, F., Darszon, A. and Visconti, P. E. (2012). Flow cytometry analysis reveals a decrease in intracellular sodium during sperm capacitation. *J. Cell Sci.* **125**, 473-485.

Ficarro, S., Chertihin, O., Westbrook, V. A., White, F., Jayes, F., Kalab, P., Marto, J. A., Shabanowitz, J., Herr, J. C., Hunt, D. F. et al. (2003). Phosphoproteome analysis of capacitated human sperm: evidence of tyrosine phosphorylation of a kinase-anchoring protein 3 and valosin-containing protein/p97 during capacitation. *J. Biol. Chem.* **278**, 11579-11589.

Fischman, K., Edman, J. C., Shackleford, G. M., Turner, J. A., Rutter, W. J. and Nir, U. (1990). A murine fer testis-specific transcript (ferT) encodes a truncated Fer protein. *Mol. Cell. Biol.* **10**, 146-153.

Gonzalez-Fernandez, L., Macias-Garcia, B., Loux, S. C., Varner, D. D. and Hinrichs, K. (2013). Focal adhesion kinases and calcium/calmodulin-dependent protein kinases regulate protein tyrosine phosphorylation in stallion sperm. *Biol. Reprod.* **88**, 138.

Goodson, S. G., Zhang, Z., Tsuruta, J. K., Wang, W. and O'Brien, D. A. (2011). Classification of mouse sperm motility patterns using an automated multiclass support vector machines model. *Biol. Reprod.* **84**, 1207-1215.

Greer, P. (2002). Closing in on the biological functions of Fps/Fes and Fer. *Nat. Rev. Mol. Cell Biol.* **3**, 278-289.

Harrison, R. A. P. (2004). Rapid PKA-catalysed phosphorylation of boar sperm proteins induced by the capacitating agent bicarbonate. *Mol. Reprod. Dev.* **67**, 337-352.

Huang, B., Wang, W., Bates, M. and Zhuang, X. (2008). Three-dimensional super-resolution imaging by stochastic optical reconstruction microscopy. *Science* **319**, 810-813.

Ijiri, T. W., Mahbub Hasan, A. K. M. and Sato, K.-I. (2012). Protein-tyrosine kinase signaling in the biological functions associated with sperm. *J. Signal Transduct.* **2012**, 181560.

Jagan Mohanarao, G. and Atreja, S. K. (2011). Identification of capacitation associated tyrosine phosphoproteins in buffalo (Bubalus bubalis) and cattle spermatozoa. *Anim. Reprod. Sci.* **123**, 40-47.

Kalab, P., Visconti, P., Leclerc, P. and Kopf, G. S. (1994). p95, the major phosphotyrosine-containing protein in mouse spermatozoa, is a hexokinase with unique properties. *J. Biol. Chem.* **269**, 3810-3817.

Khajah, M., Andonegui, G., Chan, R., Craig, A. W., Greer, P. A. and McCafferty, D.-M. (2013). Fer kinase limits neutrophil chemotaxis toward end target chemoattractants. *J. Immunol.* **190**, 2208-2216.

Kierszenbaum, A. L., Rivkin, E. and Tres, L. L. (2008). Expression of Fer testis (FerT) tyrosine kinase transcript variants and distribution sites of FerT during the development of the acrosome-acroplaxome-manchette complex in rat spermatids. *Dev. Dyn.* **237**, 3882-3891.

Kito, S. and Ohta, Y. (2008). In vitro fertilization in inbred BALB/c mice II: effects of lactate, osmolarity and calcium on in vitro capacitation. *Zygote* **16**, 259-270.

Krapf, D., Arcelay, E., Wertheimer, E. V., Sanjay, A., Pilder, S. H., Salicioni, A. M. and Visconti, P. E. (2010). Inhibition of Ser/Thr phosphatases induces capacitation-associated signaling in the presence of Src kinase inhibitors. *J. Biol. Chem.* **285**, 7977-7985.

Laemmli, U. K. (1970). Cleavage of structural proteins during the assembly of the head of bacteriophage T4. *Nature* **227**, 680-685.

Luo, J., Gupta, V., Kern, B., Tash, J. S., Sanchez, G., Blanco, G. and Kinsey, W. H. (2012). Role of FYN kinase in spermatogenesis: defects characteristic of Fyn-null sperm in mice. *Biol. Reprod.* **86**, 1-8.

Marin-Briggiler, C. I., Gonzalez-Echeverria, F., Buffone, M., Calamera, J. C., Tezon, J. G. and Vazquez-Levin, M. H. (2003). Calcium requirements for human sperm function in vitro. *Fertil. Steril.* **79**, 1396-1403.

McCafferty, D.-M., Craig, A. W. B., Senis, Y. A. and Greer, P. A. (2002). Absence of Fer protein-tyrosine kinase exacerbates leukocyte recruitment in response to endotoxin. *J. Immunol.* **168**, 4930-4935.

Mitchell, L. A., Nixon, B., Baker, M. A. and Aitken, R. J. (2008). Investigation of the role of SRC in capacitation-associated tyrosine phosphorylation of human spermatozoa. *Mol. Hum. Reprod.* **14**, 235-243.

Navarrete, F. A., Garcia-Vazquez, F. A., Alvau, A., Escoffier, J., Krapf, D., Sanchez-Cardenas, C., Salicioni, A. M., Darszon, A. and Visconti, P. E. (2015). Biphasic role of calcium in mouse sperm capacitation signaling pathways. *J. Cell. Physiol.* **230**, 1758-1769.

Okigaki, M., Davis, C., Falasca, M., Harroch, S., Felsenfeld, D. P., Sheetz, M. P. and Schlessinger, J. (2003). Pyk2 regulates multiple signaling events crucial for macrophage morphology and migration. *Proc. Natl. Acad. Sci. USA* **100**, 10740-10745.

Ovesny, M., Krizek, P., Borkovec, J., Svindrych, Z. and Hagen, G. M. (2014). ThunderSTORM: a comprehensive ImageJ plug-in for PALM and STORM data analysis and super-resolution imaging. *Bioinformatics* **30**, 2389-2390.

Parrish, J. J., Susko-Parrish, J. L. and First, N. L. (1989). Capacitation of bovine sperm by heparin: inhibitory effect of glucose and role of intracellular pH. *Biol. Reprod.* **41**, 683-699.

Porambo, J. R., Salicioni, A. M., Visconti, P. E. and Platt, M. D. (2012). Sperm phosphoproteomics: historical perspectives and current methodologies. *Expert Rev. Proteomics* **9**, 533-548.

Roy, S. C. and Atreja, S. K. (2008). Tyrosine phosphorylation of a 38-kDa capacitation-associated buffalo (Bubalus bubalis) sperm protein is induced by L-arginine and regulated through a cAMP/PKA-independent pathway. *Int. J. Androl.* **31**, 12-24.

Development (2016) 143, 2325-2333 doi:10.1242/dev.136499

Sangrar, W., Gao, Y., Scott, M., Truesdell, P. and Greer, P. A. (2007). Fer-mediated cortactin phosphorylation is associated with efficient fibroblast migration and is dependent on reactive oxygen species generation during integrin-mediated cell adhesion. *Mol. Cell. Biol.* **27**, 6140-6152.

Sangrar, W., Shi, C., Mullins, G., LeBrun, D., Ingalls, B. and Greer, P. (2015). Amplified Ras-MAPK signal states correlate with accelerated EGFR internalization, cytostasis and delayed HER2 tumor onset in Fer-deficient model systems. *Oncogene* **34**, 4109-4117.

Senis, Y. A., Craig, A. W. B. and Greer, P. A. (2003). Fps/Fes and Fer protein-tyrosinekinases play redundant roles in regulating hematopoiesis. *Exp. Hematol.* **31**, 673-681.

Shen, C. J., Raghavan, S., Xu, Z., Baranski, J. D., Yu, X., Wozniak, M. A., Miller, J. S., Gupta, M., Buckbinder, L. and Chen, C. S. (2011). Decreased cell adhesion promotes angiogenesis in a Pyk2-dependent manner. *Exp. Cell Res.* **317**, 1860-1871.

Signorelli, J., Diaz, E. S. and Morales, P. (2012). Kinases, phosphatases and proteases during sperm capacitation. *Cell Tissue Res.* **349**, 765-782.

Tang, H., Hao, Q., Fitzgerald, T., Sasaki, T., Landon, E. J. and Inagami, T. (2002). Pyk2/CAKbeta tyrosine kinase activity-mediated angiogenesis of pulmonary vascular endothelial cells. *J. Biol. Chem.* **277**, 5441-5447.

Varano, G., Lombardi, A., Cantini, G., Forti, G., Baldi, E. and Luconi, M. (2008). Src activation triggers capacitation and acrosome reaction but not motility in human spermatozoa. *Hum. Reprod.* **23**, 2652-2662.

Visconti, P. E. (2009). Understanding the molecular basis of sperm capacitation through kinase design. *Proc. Natl. Acad. Sci. USA* **106**, 667-668.

Visconti, P. E., Bailey, J. L., Moore, G. D., Pan, D., Olds-Clarke, P. and Kopf, G. S. (1995a). Capacitation of mouse spermatozoa. I. Correlation between the capacitation state and protein tyrosine phosphorylation. *Development* **121**, 1129-1137.

Visconti, P. E., Moore, G. D., Bailey, J. L., Leclerc, P., Connors, S. A., Pan, D., Olds-Clarke, P. and Kopf, G. S. (1995b). Capacitation of mouse spermatozoa. II. Protein tyrosine phosphorylation and capacitation are regulated by a cAMP-dependent pathway. *Development* **121**, 1139-1150.

Weigel, A. V., Simon, B., Tamkun, M. M. and Krapf, D. (2011). Ergodic and nonergodic processes coexist in the plasma membrane as observed by single-molecule tracking. *Proc. Natl. Acad. Sci. USA* **108**, 6438-6443.

Wertheimer, E. V., Salicioni, A. M., Liu, W., Trevino, C. L., Chavez, J., Hernandez-Gonzalez, E. O., Darszon, A. and Visconti, P. E. (2008). Chloride Is essential for capacitation and for the capacitation-associated increase in tyrosine phosphorylation. *J. Biol. Chem.* **283**, 35539-35550.

Xu, G., Craig, A. W. B., Greer, P., Miller, M., Anastasiadis, P. Z., Lilien, J. and Balsamo, J. (2004). Continuous association of cadherin with beta-catenin requires the non-receptor tyrosine-kinase Fer. *J. Cell Sci.* **117**, 3207-3219.

Yanagimachi, R., (1994). Mammalian fertilization. In *The Physiology of Reproduction* (Eds E. Knobil and J. D. Neil), pp. 189–318. New York: Raven Press.

Zeng, Y., Clark, E. N. and Florman, H. M. (1995). Sperm membrane potential: hyperpolarization during capacitation regulates zona pellucida-dependent acrosomal secretion. *Dev. Biol.* **171**, 554-563.

Zeng, Y., Oberdorf, J. A. and Florman, H. M. (1996). pH regulation in mouse sperm: identification of Na(+)-, Cl(–)-, and HCO3(–)-dependent and arylaminobenzoate-dependent regulatory mechanisms and characterization of their roles in sperm capacitation. *Dev. Biol.* **173**, 510-520.